Twenty years of giant exoplanets - Proceedings of the Haute Provence Observatory Colloquium, 5-9 October 2015
Edited by I. Boisse, O. Demangeon, F. Bouchy & L. Arnold

VLT observations of giant exoplanet atmospheres: reliability and new results

M. Lendl[1,2,3], L. Delrez[2], M. Gillon[2], N. Madhusudhan[4], E. Jehin[2], D. Queloz[3,5], D.R. Anderson[6], and C. Hellier[6]

Talk given at OHP-2015 Colloquium

[1]Space Research Institute, Austrian Academy of Sciences, Schmiedlstr. 6, 8042 Graz, Austria, (monika.lendl@oeaw.ac.at)
[2]Université de Liège, Allée du 6 août 17, Sart Tilman, Liège 1, Belgium
[3]Observatoire de Genève, Université de Genève, Chemin des maillettes 51, 1290 Sauverny, Switzerland
[4]University of Cambridge, Madingley Road, Cambridge CB3 0HA, UK
[5]Cavendish Laboratory, J J Thomson Avenue, Cambridge, CB3 0HE, UK
[6]Astrophysics Group, Keele University, Staffordshire, ST5 5BG, UK

Abstract

Transmission spectra obtained via multi-wavelength observations of transits are one of the most prominent pathways for the study of exoplanet atmospheres. We present results obtained with the ESO/VLT FORS2 instrument on the hot Saturn-mass exoplanet WASP-49b, based on three separate transit observations. FORS2 is known to produce substantial correlated noise due to inhomogeneous transparency of the telescope's linear atmospheric dispersion corrector. We account for theses systematics in a common way by using a common noise model approach. By using this approach together with low-order functions compensating for chromatic slopes, we obtain consistent results on the planetary transmission spectrum for all three dates. We do not identify any absorption signatures in the atmosphere of WASP-49b and thus conclude that this planet possesses hazes or clouds.

1 Context

Exoplanet transmission spectra can be obtained by spectrally resolved observations of planetary transits, when the stellar light is filtered through the planetary atmosphere (Seager & Sasselov 2000; Charbonneau et al. 2002). This technique has been widely used in recent years to obtain information on the properties of exoplanetary atmospheres, their compositions and structures. At optical and near-infrarecd wavelengths, the prominent absorption signatures of H_2O, Na and K, and also the Rayleigh scattering signature of H_2 have been identified in a number of planets (e.g., Charbonneau et al. 2002; Redfield et al. 2008; Lecavelier Des Etangs et al. 2008; Sing et al. 2011, 2015; Deming et al. 2013; Huitson et al. 2013). Such observations have also revealed that many planets possess transmission spectra with suppressed absorption features, a property likely caused by the presence of clouds or hazes that contribute a mostly gray opacity (e.g., Pont et al. 2008; Gibson et al. 2013; Sing et al. 2013). In some cases, the molecular and elemental signatures are nearly completely obscured, indicating the absorbing cloud or haze layer is located at high altitudes in the planetary atmosphere where it efficiently obscures the atmosphere below.

Recent observing campaigns have made extensive use of the space-based HST STIS and WFC3 instruments, detecting the signatures of Na, K, and H_2O in a number of objects (see Crossfield 2015; Sing et al. 2016 and references therein). Ground-based observatories have contributed to these studies with multi-object spectrographs such as FORS2 (e.g., Bean et al. 2010, 2011), GMOS (e.g., Gibson et al. 2013; Stevenson et al. 2014) and OSIRIS (e.g., Murgas et al. 2014).

We show results for the planet WASP-49b (Lendl et al. 2012), a low-density Saturn-mass planet orbiting a G6 V star every 2.78 days. We made use of the FORS2 (Appenzeller et al. 1998) instrument, a multi-purpose optical imager and spectrograph installed at the ESO VLT/UT1. Until its upgrade in 2014, high-precision (spectro-)photometry with FORS2 was affected by large correlated noise due to inhomogeneities of the telescope's linear atmospheric dispersion corrector (LADC) (Moehler et al. 2010). Our observations fall into this period.

2 VLT/FORS2 observations, analysis, and noise models

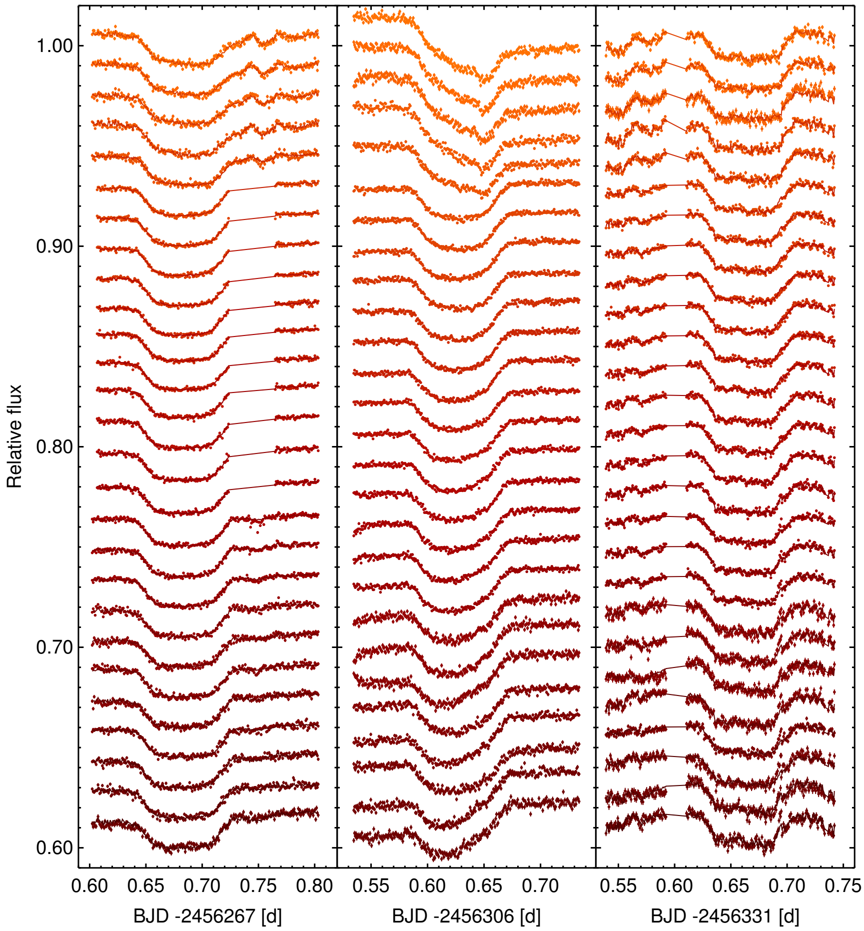

Figure 1: Wavelength-binned FORS2 transit lightcurves of WASP-49. The wavelength of the individual light curves increases from top to bottom, and the bin centers are 743, 753, 763, 773, 783, 793, 803, 813, 823, 833, 843, 853, 863, 873, 883, 893, 903, 913, 923, 933, 943, 953, 963, 973, 983, 994, and 1010 nm.

We obtained spectrophotometric observations with FORS2 throughout three transits of WASP-49b between December 2012 and February 2013. During the observations, we set the LADC's prism separation to constant to limit differential effects from the LADC-induced red noise. The lightcurves were obtained via differential spectrophotometry using all available reference stars (that is, two reference stars for the five shortest-wavelength bands, and three reference stars for all others) and are shown in Figure 1. They show characteristic wave-like features at the meridian passage (at BJD-2456000 values of 267.75, 306.65, and 331.56), that are due to rapid rotation of the LADC across the field of view. We analyze the lightcurves together with a set of 10 additional broad-band photometric lightcurves obtained from EulerCam (Lendl et al. 2012, *r'* and *NGTS* filters) and TRAPPIST (Gillon et al. 2011; Jehin et al. 2011, *I*+*z'* filter).

We performed a markov chain monte carlo (MCMC) analysis, using a modified version of the code described in Gillon, M. et al. (2012). To model the substantial LADC-induced correlated noise in the FORS2 lightcurves, we devised a common noise model (CNM) for lightcurves affected with the same noise structure (i.e., lightcurves obtained on the same date and reference stars). The CNM is calculated by co-adding the residuals of the contributing lightcurves at each MCMC step while fixing the transit depth to a previously-determined "white" value. This method is similar, but not identical, to the "divide-white" method that uses white light curves for the definition of the correlated noise component (e.g., Stevenson et al. 2014).

We tested three modeling approaches for the reliability of the inferred transmission spectrum:

- Parametric functions as photometric baseline models: polynomials up to fourth order in the parallactic angle *par*, *cos*(*par*), or its change *dpar*
- The CNM alone
- Simple Parametric functions (i.e., maximally a second-order polynomial in the parallactic angle) together with the CNM

We find that the transmission spectra observed at the three epochs only agree if the CNM is used together with low-order polynomials which are needed to compensate for color-dependent lightcurve slopes. This is illustrated in Figure 2. Note that using the CNM alone creates a false slope in the transmission spectrum of 14 January 2013. On the other hand, using high-order parametric functions unnecessarily inflates the error bars as common systematics are fit individually, and we observe slight offsets between lightcurves analyzed with different baseline functions.

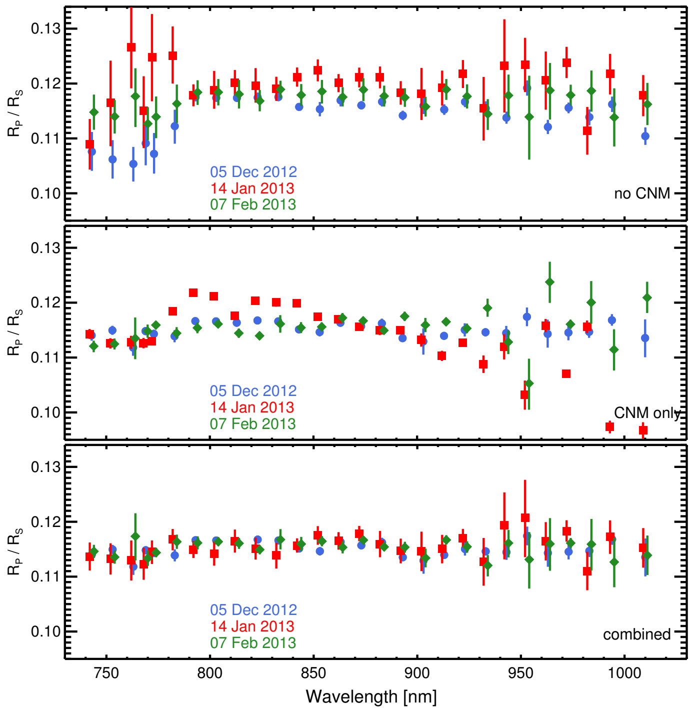

Figure 2: The transmission spectra of the three separate transit observations resulting from different treatments of correlated noise. The top panel shows the result if complicated parametric functions are used, the middle panel that of the CNM-only analysis, and the bottom panel shows the result obtained by using the CNM together with low-order polynomials.

3 The transmission spectrum of WASP-49b

To improve the overall precision of the transmission spectrum, we use the combined approach and perform a global analysis of all three transits and the supplementary broadband data, allowing for only one transit depth per wavelength bin. The resulting transmission spectrum of WASP-49b is shown in Figure 3, and compared to four model spectra:

- a clear Solar-composition atmosphere

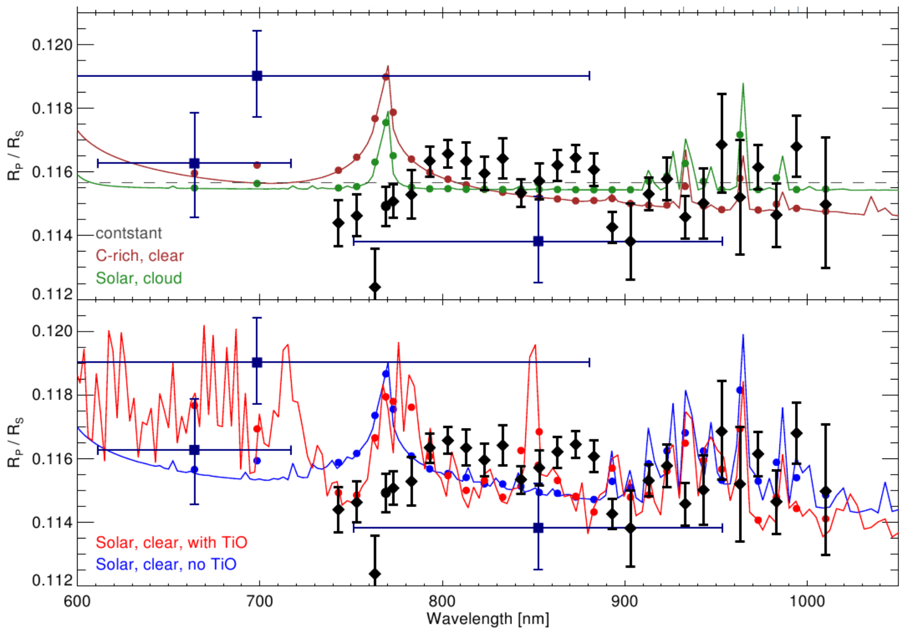

Figure 3: The transmission spectrum of WASP-49b from FORS2 (black diamonds), together with the broadband measurements from EulerCam and TRAPPIST (blue squares). The model spectra shown are those of a clear Carbon-rich (top panel, red), a cloudy Solar-composition (top panel, green), and a clear Solar-composition with (bottom panel, red), and without (bottom panel, blue) TiO. A flat spectrum is indicated as a dashed line in the top panel.

- a Solar-composition atmosphere with a cloud deck at 10 mbar altitude
- a clear Solar-composition atmosphere including TiO
- a Carbon-rich atmosphere

These model atmospheres have been calculated following the procedures of Madhusudhan & Seager (2009) and Madhusudhan (2012). We also compared the observed transmission spectrum to a horizontal line as would be produced by a spectrum where the features are completely obscured by high-altitude clouds or hazes. We find that flatter models, i.e., the cloudy Solar-composition and the Carbon-rich model fit well, but the best match is given by the featureless spectrum. We find no indication of either potassium or water absorption; WASP-49b appears to be a hot giant planet with a significant cloud or haze component in its atmosphere.

Acknowledgments: This work was supported by the European Research Council through the European Union's Seventh Framework Programme (FP7/2007-2013)/ERC grant agreement number 336480. TRAPPIST is funded by the Belgian Fund for Scientific Research (Fond National de la Recherche Scientifique, FNRS) under the grant FRFC 2.5.594.09.F, with the participation of the Swiss National Science Fundation (SNF). L. Delrez acknowledges the support of the F.R.I.A. fund of the FNRS. M. Gillon and E. Jehin are FNRS Research Associates.

References

Appenzeller, I., Fricke, K., Fürtig, W., et al. 1998, The Messenger, 94, 1

Bean, J. L., Désert, J.-M., Kabath, P., et al. 2011, ApJ, 743, 92

Bean, J. L., Miller-Ricci Kempton, E., & Homeier, D. 2010, Nature, 468, 669

Charbonneau, D., Brown, T. M., Noyes, R. W., & Gilliland, R. L. 2002, ApJ, 568, 377

Crossfield, I. J. M. 2015, PASP, 127, 941

Deming, D., Wilkins, A., McCullough, P., et al. 2013, ApJ, 774, 95

Gibson, N. P., Aigrain, S., Barstow, J. K., et al. 2013, MNRAS, 436, 2974

Gillon, M., Jehin, E., Magain, P., et al. 2011, Detection and Dynamics of Transiting Exoplanets, St. Michel l'Observatoire, France, Edited by F. Bouchy; R. Díaz; C. Moutou; EPJ Web of Conferences, Volume 11, id.06002, 11, 6002

Gillon, M., Triaud, A. H. M. J., Fortney, J. J., et al. 2012, A&A, 542, A4

Huitson, C. M., Sing, D. K., Pont, F., et al. 2013, MNRAS, 434, 3252

Jehin, E., Gillon, M., Queloz, D., et al. 2011, The Messenger, 145, 2

Lecavelier Des Etangs, A., Vidal-Madjar, A., Désert, J.-M., & Sing, D. 2008, A&A, 485, 865

Lendl, M., Anderson, D. R., Collier-Cameron, A., et al. 2012, A&A, 544, A72

Madhusudhan, N. 2012, ApJ, 758, 36

Madhusudhan, N. & Seager, S. 2009, ApJ, 707, 24

Moehler, S., Freudling, W., Møller, P., et al. 2010, PASP, 122, 93

Murgas, F., Pallé, E., Zapatero Osorio, M. R., et al. 2014, A&A, 563, A41

Pont, F., Knutson, H., Gilliland, R. L., Moutou, C., & Charbonneau, D. 2008, MNRAS, 385, 109

Redfield, S., Endl, M., Cochran, W. D., & Koesterke, L. 2008, ApJ, 673, L87

Seager, S. & Sasselov, D. D. 2000, ApJ, 537, 916

Sing, D. K., Désert, J.-M., Fortney, J. J., et al. 2011, A&A, 527, A73

Sing, D. K., Fortney, J. J., Nikolov, N., et al. 2016, Nature, 529, 59–62

Sing, D. K., Lecavelier des Etangs, A., Fortney, J. J., et al. 2013, MNRAS, 436, 2956

Sing, D. K., Wakeford, H. R., Showman, A. P., et al. 2015, MNRAS, 446, 2428

Stevenson, K. B., Bean, J. L., Seifahrt, A., et al. 2014, AJ, 147, 161